

# Decay mechanism of $^{264}_{104}\text{Rf}^*$ superheavy nucleus formed in $^{238}_{92}\text{U} + ^{26}_{12}\text{Mg}$ reaction

Gurjit Kaur, Neha Sharma, and Manoj K. Sharma\*

\*School of Physics and Materials Science,

Thapar Institute of Engineering and Technology, Patiala-147004, India.

## Introduction

Heavy ion induced reactions provide an essential tool for the production of stable compound nuclear systems. But with increase in charge/mass number of projectile and target, the synthesis of heavier nuclei becomes difficult due to the dominance of strong dissipative forces. In superheavy mass region, such effects become more pronounced as the repulsive forces between interacting massive nuclei can lead to non-compound nuclear mechanisms such as quasi-fission (QF) which hinders the formation of compound nucleus [1]. The knowledge of possible emergence of different fission processes like fusion-fission and quasi-fission can provide important information about the survival of superheavy nuclear systems against prompt disintegration.

In the previous study of dynamical cluster decay model (DCM) [2], the excitation functions for evaporation residues of  $^{266}\text{Rf}^*$  formed in  $^{248}\text{Cm} + ^{18}\text{O}$  reaction [3] were addressed but the fission channel of the same was not explored. So in the present work, an attempt is made to address the neutron evaporation and fission dynamics of  $^{264}\text{Rf}^*$  superheavy nucleus formed in  $^{238}\text{U} + ^{26}\text{Mg}$  reaction. The experimentally available neutron evaporation and fission decay data [4] is addressed using  $\beta_2$ -deformations and optimum orientations within DCM framework. Also, an attempt is made to predict the fission cross-sections around the Coulomb barrier energies. Further, the decay profile is explored in terms of preformation yield which suggests the symmetric fission distribution of  $^{264}\text{Rf}^*$  superheavy nucleus. At last, the survival probabilities ( $W_{Sur}$ ) of evaporation residue channels against fission are estimated.

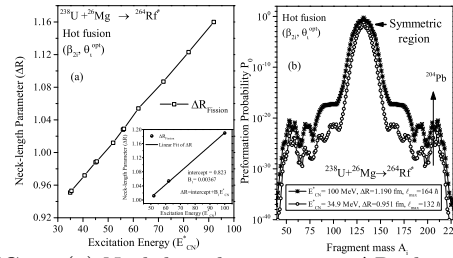


FIG. 1: (a) Neck-length parameter  $\Delta R$  plotted as a function of excitation energy for  $^{264}\text{Rf}^*$  nucleus to extend the fission cross-sections for unknown region. Inset shows the linear curve fitting of  $\Delta R$  values obtained from experimental data. (b) Preformation yield plotted as a function of fragment mass ( $A_i$ ) at two extreme fission energies.

## The Model

The dynamical cluster decay model [2] based on fragmentation theory is worked out in terms of mass/charge asymmetry, relative separation  $\bar{R}$ , neck parameter, temperature, deformation [5] and orientation. In terms of these parameters the Schrödinger wave equation is solved in  $\eta$ -coordinates at fixed  $R=R_a$  to get the preformation probability ( $P_0$ ) as

$$P_0 = |\psi(\eta(A_i))|^2 \sqrt{B_{\eta\eta}} \frac{2}{A_{CN}} \quad (1)$$

The barrier penetrability ( $P$ ) of the decaying fragments is worked out using WKB approach [2]. Finally, in term of  $P_0$  and  $P$ , the compound nucleus decay cross-sections for  $\ell$ -partial waves is calculated as

$$\sigma = \frac{\pi}{k^2} \sum_{\ell=0}^{\ell_{max}} (2\ell + 1) P_0 P; \quad k = \sqrt{\frac{2\mu E_{c.m.}}{\hbar^2}} \quad (2)$$

## Calculations and Results

Fig.1(a) shows the variation of neck-length parameter ( $\Delta R$ ) for fission data as a function of excitation energy ( $E_{CN}^*$ ). The  $\Delta R$  values obtained by fitting the experimental

TABLE I: The DCM fitted fission cross-sections in comparison to experimental data [4] for the decay of  $^{264}\text{Rf}^*$  nuclear system. The DCM predicted cross-sections for unexplored region are also shown in this table.

$E_{CN}^*$ (MeV)	$E_{c.m.}$ (MeV)	$\Delta R$ (fm)	$\ell_{max}$ ( $\hbar$ )	$\sigma_{Fission}^{DCM}$ (mb)	$\sigma_{Fission}^{Exp.}$ (mb)
34.9	110.9	0.951	132	2.17	-
35.4	111.4	0.953	132	2.97	-
40.6	116.6	0.972	134	14.60	-
45.0	121.4	0.988	136	32.54	-
45.4	121.4	0.989	137	40.77	-
52.0	127.0	1.012	139	94.0	95±30
56.0	132.0	1.028	140	117.2	-
56.2	132.2	1.029	140	135.0	-
62.0	127.0	1.054	142	268.0	270±80
72.0	148.0	1.087	143	346.4	-
82.0	158.0	1.123	148	467.5	-
92.0	168.0	1.160	152	501.1	-
100.0	176.0	1.190	164	854.0	910±300

fission data at different energies are shown in the inset of Fig.1(a) and a linear increase in neck-length values is observed as a function of excitation energy. This linear curve gives a relation between  $E_{CN}^*$  and  $\Delta R$  as  $\Delta R = \text{intercept} + B_1 E_{CN}^*$ . Here,  $\text{intercept} = 0.823$  and constant  $B_1 = 0.00367$ . Further to predict the fission cross-sections around the Coulomb barrier, the values of neck-length parameter at respective energies are extrapolated using above relation. With the help of these values of  $\Delta R$  at different energies, the fission cross-sections are predicted using DCM for unexplored region as shown in Table I. The fission cross-sections show increment with increase in excitation energy which indicate higher chances of fission for higher excited compound system.

Further, the preformation probability ( $P_0$ ) as a function of fragment mass is plotted in Fig.1(b) for  $^{264}\text{Rf}^*$  compound system at two extreme excitation energies. Symmetric mass distribution of fragments is observed for reaction under consideration indicating that fusion-fission is the prime decay mode. The preformation probabilities ( $P_0$ ) of the fragments in the mass range of  $A/2 \pm 20$  is significantly high as compare to relatively lower

mass fragments. The possible reason for the symmetric division of the fragments is the influence of deformations on the underlying potential which favors mass drift toward symmetric fission. In addition to the symmetric fission, the secondary peaks around  $^{204}\text{Pb}$  are also observed in heavy mass fragment (HMF) region but the contribution of these Pb-peaks is very small in comparison to symmetric fragments. The presences of Pb-peaks in HMF region of superheavy nuclei are generally related with the quasi-fission phenomenon, which seems negligible in the present case. In addition to this, the experimentally available evaporation residues (ER) [4] cross-sections are also fitted by DCM and these fitted ER and fission cross-sections are used to calculate the survival probabilities of  $3n$ ,  $4n$ ,  $5n$ , and  $6n$  evaporation channels over fission which are not shown here. A careful study and comparison of the  $W_{Sur}$  values for neutrons evaporation suggest that for higher energies the compound nucleus stabilizes via emission of heavier neutron cluster.

### Acknowledgments

The financial support from the DST, New Delhi in the form of INSPIRE-fellowship (grant no. DST/INSPIRE/03/2015/000199) is gratefully acknowledged.

### References

- [1] Y. Aritomo and M. Ohta, Nucl. Phys. A **744**, 3-14 (2004); M. G. Itkis *et al.* Nucl. Phys. A **944**, 204-237 (2015); E. M. Kozulin *et al.*, Phys. Rev. C **94**, 054613 (2016).
- [2] G. Kaur, K. Sandhu, and M. K. Sharma, Phys. Rev. C **97**, 054602 (2018).
- [3] K. Sandhu, M. K. Sharma, A. Kaur, and R. K. Gupta, Phys. Rev. C **90**, 034610 (2014).
- [4] J. M. Gates *et al.* Phys. Rev. C **77**, 034603 (2008); W. Q. Shen *et al.*, Phys. Rev. C **36**, 115-142 (1987).
- [5] P. Möller, J. R. Nix, W. D. Myers, and W. J. Swiatecki, At. Data Nucl. Data Tables **59**, 185 (1995).